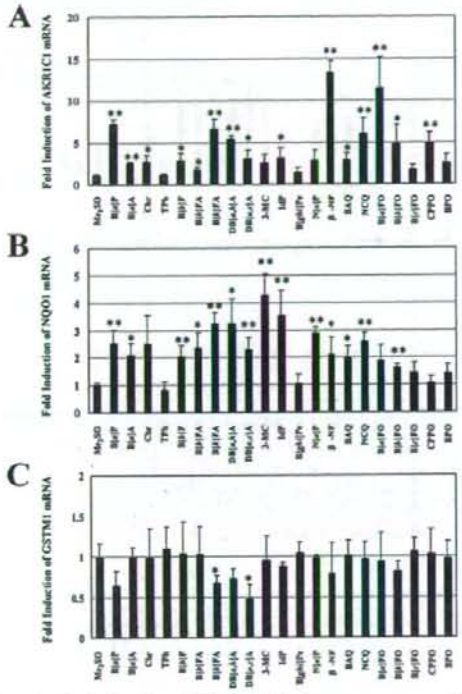

Figure 3. Induction for mRNA of metabolic enzymes measured by RT-PCR in HepG2 cells exposed to 5 μM PAHs and oxy-PAHs for 24 h. (A) AKR1C1 mRNA, (B) NQO1 mRNA, and (C) GSTM1 mRNA were measured. Two asterisks (**) indicate a highly significant difference from control ($p < 0.01$), and one asterisk (*) indicates a significant difference from control ($p < 0.05$) as determined by a *t*-test.

The ratio of NQO1 mRNA levels to GAPDH mRNA of Me_2SO control level was 2.4×10^{-1}. NQO1 mRNA levels were high for 3-MC and IdP (both were 4-fold to control), and B[*a*]P, Chr, B[*k*]FA, DB[*a,h*]A, N[*a*]P, and NCQ all were 3-fold (Figure 3B). The ratio of GSTM1 mRNA levels to GAPDH mRNA of Me_2SO control level was 8.4×10^{-2}. No test chemical induced GSTM1 mRNA significantly. However, GSTM1 mRNA levels of B[*a*]P, B[*k*]FA, DB[*a,h*]A, and DB-[*a,c*]A were lower than the control level (0.6-, 0.7-, 0.7-, and 0.5-fold, respectively) (Figure 3C).

Dose-Dependent Induction of mRNA of Metabolic Enzymes after Exposure to PAHs and Oxy-PAHs for 24 h. The concentration-dependent induction of P450s, NQO1, and GSTM1 mRNA exposed for 24 h to B[*a*]P, B[*k*]FA, DB[*a,h*]A, IdP, NCQ, and B[*b*]FO was also examined (Figure 4). The EC_{25} for the TCDD-dependent induction of P4501A1 mRNA in HepG2 cells was 68 pM (Figure 4A and Table 1). B[*a*]P was approximately 2000-fold less potent than TCDD. Also, in this experiment, PAHs such as B[*k*]FA and DB[*a,h*]A induced P4501A1 mRNA transcription much more strongly than B[*a*]P (100- and 6.7-fold IEF, respectively). Oxy-PAHs, NCQ, and B[*b*]FO induced P4501A1 mRNA transcription less strongly than B[*a*]P; nevertheless, these activities are considered to be high (0.66- and 0.58-fold IEF, respectively). Dose–response curves of P4501A2 mRNA inductions for the six compunds were quite similar to P4501A1, respectively (Figure 4B).

The order of the strength for NQO1 mRNA induction judged from the dose–response curves was as follows, B[*k*]FA, DB-[*a,h*]A, IdP > B[*a*]P, NCQ > B[*b*]FO, and slight NQO1 mRNA induction by 1.6 nM TCDD seemed to be observed (Figure 4C). GSTM1 mRNA induction was slightly decreased by concentration over 500 nM for B[*a*]P and B[*k*]FA and over 5 μM for DB[*a,h*]A and B[*b*]FO (Figure 4D).

Time-Dependent Induction for mRNA of Metabolic Enzymes after Exposure by 5 μM PAHs and Oxy-PAHs. Time–course induction levels of P4501A1, AKR1C1, NQO1, and GSTM1 mRNA by six representative 5 μM PAHs and oxy-PAHs (B[*a*]P, B[*k*]FA, DB[*a,h*]A, IdP, NCQ, and B[*b*]FO) were also examined (Figure 5). The induction of P4501A1 mRNA increased rapidly after exposure for six all PAHs and oxy-PAHs (Figure 5A) and was especially remarkable and continued through 48 h for B[*k*]FA and DB[*a,h*]A. Induction levels were almost constant after 6 h for NCQ and B[*b*]FO.

The mRNA induction of AKR1C1 increased quickly from 6 to 24 h for all PAHs and oxy-PAHs. The increase in rate for mRNA induction of AKR1C1 was higher for oxy-PAHs, NCQ, and B[*b*]FO than for nonoxy-PAHs (Figure 5B). The observed tendency was that the induction of AKR1C1 mRNA for all of the compounds started to decrease after 24 h.

The mRNA induction of NQO1 increased slowly at first but rose quickly from 6 to 24 h for most PAHs and oxy-PAHs. The increase in rate for the mRNA induction of NQO1 was slightly higher for oxy-PAHs, NCQ, and B[*b*]FO than for nonoxy-PAHs (Figure 5C). The induction of NQO1 mRNA started to decrease from about 24 h after for B[*a*]P, NCQ, and B[*b*]FO and was constant from 24 to 72 h for B[*k*]FA, DB-[*a,h*]A, and IdP. The observed tendency for GSTM1 mRNA showed slight decreases in induction for all PAHs and oxy-PAHs until 12 h. This tendency continued until 48 h for B[*a*]P and B[*k*]FA; however, the induction levels started to increase again after 12 h and exceeded control levels for B[*b*]FO, NCQ, IdP, and DB[*a,h*]A (Figure 5D).

Discussion

Some of the main target organs for carcinogenesis by PAHs include lung, skin, and mammary glands; for example, mammal hepatoma cells are often used for examining metabolic enzyme induction and DNA adduct formation by PAHs such as B[*a*]P because the liver induces various metabolic enzymes at relatively high levels. It has also been suggested that liver metabolism plays a role for detoxification of PAHs and oxy-PAHs in local carcinogenesis; therefore, liver cells are appropriate for examining the induction patterns of enzymes related to detoxification.

Several research groups have reported induction of P4501A1 by PAHs in HepG2 cells (*12*, *30*, *35*–*40*), and the order for the strength of the induction was as follows: B[*k*]FA > DB[*a,h*]A > IdP > B[*b*]FA > B[*a*]P > Chr, B[*a*]A. This was determined from data utilizing the luciferase assay after 16 h and the immunoblot assay after 24 h (*37*, *39*). These patterns were similar to our RT-PCR results after 24 h (Figure 4A). In this study, the levels of induction of P4501A1 mRNA by all 5 μM-dosed PAHs and oxy-PAHs did not decrease even after HepG2 cells were continually exposed for 72 h (Figure 5A). The mRNA half-life of P4501A1 is short (2.4 h), while the half-lives of both P4501A2 and P4501B1 mRNA are more than 24 h (*41*). It was reported that more than 75% of approximately 2 μM B[*a*]P was metabolized for 24 h in HepG2 cells and the tendency of metabolism for B[*k*]FA was similar to B[*a*]P (*37*, *42*). Penning et al. suggested that one of the oxygenated metabolites of B[*a*]P, *o*-quinone (BPQ), also contributed to P4501A1 induction in HepG2 cells exposed to B[*a*]P. Therefore, it is possible that some oxygenated metabolites of B[*k*]FA contrib-

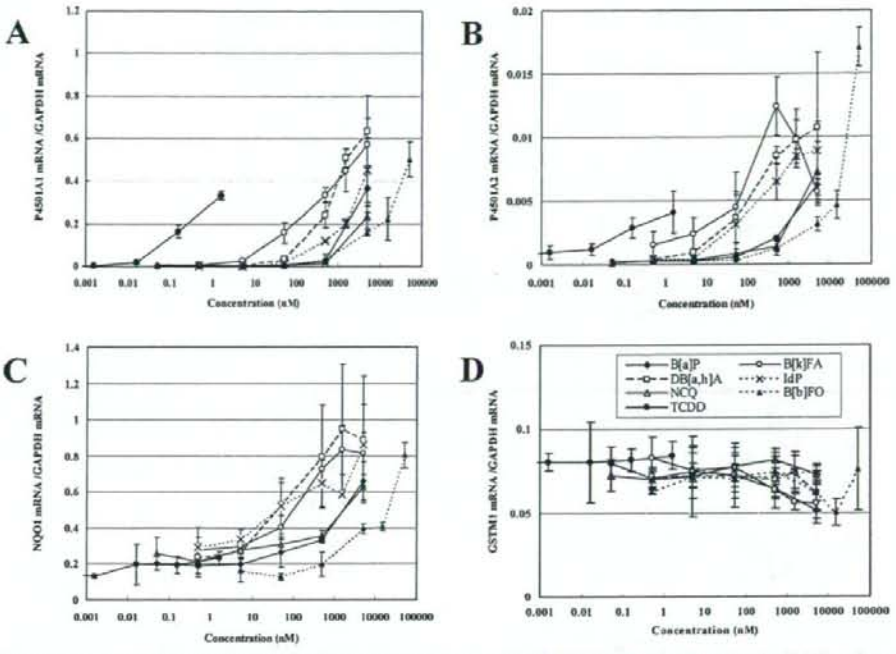

Figure 4. Dose-dependent induction for mRNA of metabolic enzymes measured by RT-PCR in HepG2 cells exposed to PAHs and oxy-PAHs for 24 h. (A) P4501A1 mRNA, (B) P4501A2 mRNA, (C) NQO1 mRNA, and (D) GSTM1 mRNA were measured.

Table 1. P4501A1 mRNA Induction in HepG2 Cells (for 24 h) by PAHs, oxy-PAHs, and TCDD

compound	EC_{TCDD25} (nM)[a]	IEF[b]
B[*a*]P	1.3×10^3	1
B[*k*]FA	13	100
DB[*a,h*]A	200	6.7
IdP	350	3.8
NCQ	2.0×10^3	0.66
B[*b*]FO	2.3×10^3	0.58
TCDD	0.068	1.9×10^4

[a] Concentration equivalent with 25% of TCDD max (P4501A1 mRNA induction). [b] IEF relative to B[*a*]P (P4501A1 mRNA induction).

uted to the strong AhR-mediated induction of P4501A1 mRNA even after 72 h (*12*). It was shown that many DNA adducts caused by oxygenated metabolites such as hydroxyepoxides and bisdiols were formed when animals or culture cells were exposed to IdP and DB[*a,h*]A (*43*, *44*). Indeed, high levels of formation of oxygenated metabolites may explain the strong P4501A1 mRNA induction for IdP and DB[*a,h*]A even after 72 h. In the case of oxy-PAHs NCQ and B[*b*]FO, continual P4501A1 mRNA induction, even after 72 h, may have been generated by oxygenated metabolites or ROS formation. The study for examining these possibilities is underway.

Penning et al. reported that the induction of AKR1C1 mostly occurred in four human isoforms of AKRs (AKR1C1–AKR1C4) when HepG2 cells and human colon carcinoma (HT29) cells were exposed to antioxidants such as β-NF and *tert*-butylhydroquinone and ROS such as H_2O_2 (*13*). They reported also that *trans*-dihydrodiols of some PAHs (naphthalene, phenanthrene, B[*a*]A, Chr, B[*a*]P, etc.) were converted to PAH catechols by several AKRs (*21*). In our study, the mRNA induction levels of AKR1C1 were significantly high at the exposure to 5 μM oxy-PAHs such as NCQ, B[*a*]FO, B[*b*]FO, CPPO, and β-NF (Figure 3A). The rapid increase for the induction of AKR1C1 mRNA via activated AP-1 was observed for oxy-PAHs NCQ and B[*b*]FO (Figure 5B); therefore, it is possible that these compounds themselves are AP-1 active compounds and AKR1C1 inducers. P450s-inducing PAHs such as B[*a*]P, B[*k*]FA, and DB[*a,h*]A at 5 μM also induced AKR1C1 mRNA significantly for 24 h, and the start of AKR1C1 mRNA inductions for B[*a*]P, B[*k*]FA, and DB[*a,h*]A required more than 6 h. Therefore, it is suggested that some P4501A1-catalyzed electrophilic oxygenated metabolites of PAHs (Michael reaction acceptors) or ROS generated from these metabolites contributed to the induction of AKR1C1 mRNA (Figures 2, 3A, and 5B).

Cytosolic NQO1 is the enzyme that catalyzes two-electron reduction and detoxification of quinones, repressing one-electron reduction of quinones by microsomal NADPH-dependent cytochrome P450 reductase and mitochondrial NADH-dependent ubiquinone oxidoreductase (*9*, *15–17*, *21*, *28*, *29*, *45*). Several PAH quinones were reduced via both one- and two-electron reductions (*21*, *29*). In our study, the mRNA induction levels of NQO1 were high after PAH exposure for 24 h at 5 μM except for TPh and B[*ghi*]Pe and this pattern is similar to P4501A1 and 1A2. However, the point that oxy-PAHs such as BAQ, NCQ, B[*a*]FO, B[*b*]FO, and β-NF at 5 μM induced NQO1 mRNA at the same levels as these nonoxy-PAHs was different from the patterns of P4501A1 and 1A2 mRNA induction. The tendency for a rapid increase in NQO1 mRNA induction from 6 h for most PAHs and oxy-PAHs is similar to AKR1C1 and the slightly higher rate increase of NQO1 mRNA induction for oxy-PAHs, NCQ, and B[*b*]FO, more than for nonoxy-PAHs, is also similar to AKR1C1 (Figure 5C). That the induction of NQO1 mRNA did not decrease from 24 to 72 h for B[*k*]FA, DB[*a,h*]A, and IdP is similar to P4501A1. NQO1 is regulated by both XRE (AhR) and EpRE (AP-1), so the result of the induction of NQO1 mRNA is thought to be the mixed type of

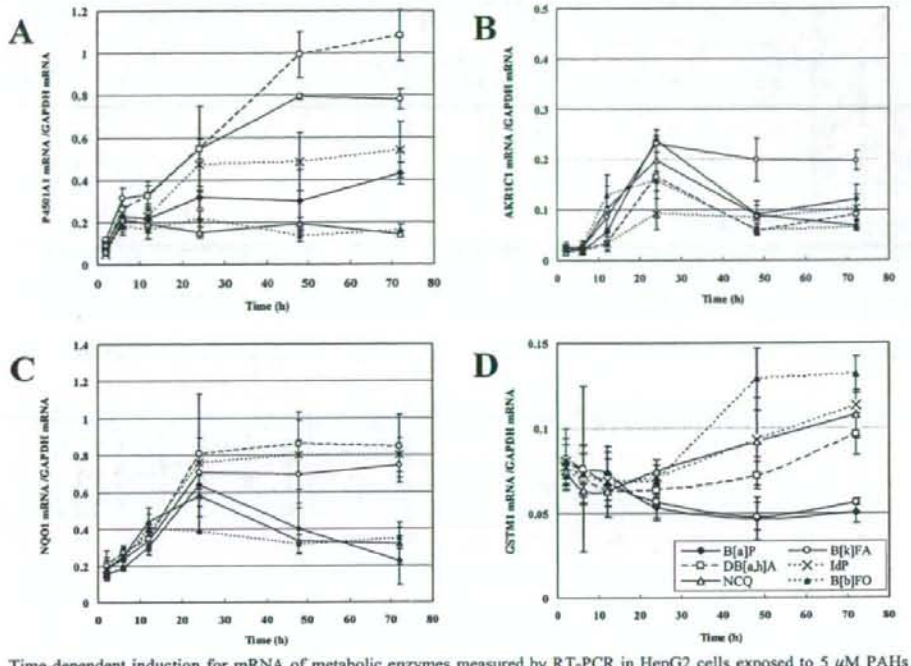

Figure 5. Time-dependent induction for mRNA of metabolic enzymes measured by RT-PCR in HepG2 cells exposed to 5 μM PAHs and oxy-PAHs. (A) P4501A1 mRNA, (B) AKR1C1 mRNA, (C) NQO1 mRNA, and (D) GSTM1 mRNA were measured.

P4501A1 mRNA and AKR1C1 mRNA based upon chemical dependency and time-dependent curves (Figures 2, 3, and 5). The contribution to NQO1 mRNA induction via EpRE (electrophiles or ROS) may be more than the contribution by AhR because the promoter of the human *NQO1* gene contains an imperfect XRE (*17*).

GSTAs, GSTMs, GSTPs, and GSTTs are included in human isoenzymes of GST (*17*, *46*, *47*). These GSTs catalyze GSH conjugation with ROS or B[*a*]P metabolites such as epoxides (BPDE, etc.) and quinones (BPQ, etc.) (*12*, *17*, *21*, *48*). In HepG2 cells exposed to a Me_2SO control and some PAHs and oxy-PAHs, the mRNA levels of GSTA1 and GSTP1 were at least two magnitudes lower than GSTM1 in additional RT-PCR (data not shown); so, in this study, the GSTM1 isoform was measured in detail (*42*, *47*). The frequency of deficiency of the *GSTM1* gene is higher than other *GST* genes in humans (*14*, *17*), and the promoter of the *GSTM1* gene also contains both XRE and EpRE (*17*); however, in this study, mRNA induction was not dramatically increased by any PAH and oxy-PAH. Although the tendency for decrease in GSTM1 mRNA in the dose−response curves for several PAHs and oxy-PAHs and in the time−course curve for all PAHs and oxy-PAHs was observed and these decreases were much greater for B[*a*]P and B[*k*]FA, the mechanism of these phenomena was not clear (Figures 4D and 5D). It may be derived from a shortage of GSH during reactions with ROS or diolepoxides (*49*).

In conclusion, the pattern for induction of metabolic enzymes by three nonoxy-PAHs (B[*k*]FA, DB[*a*,*h*]A, and IdP) was similar to B[*a*]P. Considering this, mechanisms of metabolism by them are possibly similar to B[*a*]P. In the case of oxy-PAHs, the general mechanisms of induction of metabolic enzymes may be similar to that of quinone-yielding ROS (*21*, *45*). It will be necessary to examine the relationships between metabolite formation of PAHs and oxy-PAHs and DNA adduct formation and metabolic enzyme induction by them in detail. Additionally, it will be interesting to examine the patterns of metabolic enzyme induction and DNA adduct formation after compound exposure by using target organ cells in carcinogenesis studies in the future.

Acknowledgment. We thank Robert Kanaly, Department of Environmental Biosciences and International Graduate School of Arts and Sciences, Yokohama City University, Yokohama, Japan, for help in manuscript preparation. This work was supported in part from the Ministry of Health, Labour and Welfare and Grants-in-Aid for Scientific Research on Priority Areas (13027245, 16201012, and 18101003) from the Japanese Ministry of Education, Science, Sports and Culture.

References

(1) Hannigan, M. P., Cass, G. R., Penman, B. W., Crespi, C. L., Lafleur, A. L., Busby, W. F., Jr., Thilly, W. G., and Simoneit, B. R. T. (1998) Bioassay-directed chemical analysis of Los Angeles airborne particulate matter using a human cell mutagenicity assay. *Environ. Sci. Technol. 32*, 3502−3514.

(2) Rogge, W. F., Hildemann, L. M., Mazurek, M. A., and Cass, G. R. (1993) Sources of fine organic aerosol. 2. Noncatalyst and catalyst-equipped automobiles and heavy-duty diesel trucks. *Environ. Sci. Technol. 27*, 636−651.

(3) Alsberg, T., Strandell, M., Westerholm, R., and Stenberg, U. (1985) Fractionation and chemical analysis of gasoline exhaust particulate extracts in connection with biological testing. *Environ. Int. 11*, 249−257.

(4) Fernandez, P., and Bayona, J. M. (1992) Use of off-line gel permeation chromatography-normal-phase liquid chromatography for the determination of polycyclic aromatic compounds in environmental samples and standard reference materials (air particulate matter and marine sediment). *J. Chromatogr. 625*, 141−149.

(5) IARC. (1983) Polynuclear aromatic compounds, Part 1. Chemical, environmental and experimental data. *IARC Monographs on the Evaluation of the Carcinogenic Risk of Chemicals to Humans*, Vol. *32*. IARC, Lyon, France.

(6) Monarca, S., Feretti, D., Zanardini, A., Moretti, M., Villarini, M., Spiegelhalder, B., Zerbini, I., Gelatti, U., and Lebbolo, E. (2001) Monitoring airborne genotoxicants in the rubber industry using genotoxicity tests and chemical analysis. *Mutat. Res. 490*, 159−169.
(7) Straif, K., Baan, R., Grosse, Y., Secretan, B., Ghissassi, F. E., and Cogliano, V. (2005) Carcinogenicity of polycyclic aromatic hydrocarbons. *Lancet Oncol. 6*, 931−932.
(8) Durant, J. L., Busby, W. F., Jr., Lafleur, A. L., Penman, B. W., and Crespi, C. L. (1996) Human cell mutagenicity of oxygenated, nitrated and unsubstituted polycyclic aromatic hydrocarbons associated with urban aerosols. *Mutat. Res. 371*, 123−157.
(9) Pelkonen, O., and Nebert, D. W. (1982) Metabolism of polycyclic aromatic hydrocarbons: Ethiologic role in carcinogenesis. *Pharmacol. Rev. 34*, 189−222.
(10) Møller, L., Hagen, I., and Ramdahl, T. (1985) Mutagenicity of polycyclic aromatic compounds (PAC) identified in source emissions and ambient air. *Mutat. Res. 157*, 149−156.
(11) Tada, K., Odashima, N., and Ishidate, M. (1966) On the screening experiment for the carcinogenesis of polycyclic quinones. *Kyoritsu Pharm. Univ. Environ. Doc.* 63−68.
(12) Burczynski, M. E., and Penning, T. M. (2000) Genotoxic polycyclic aromatic hydrocarbon *ortho*-quinones generated by aldo-keto reductases induce CYP1A1 via nuclear translocation of the aryl hydrocarbon receptor. *Cancer Res. 60*, 908−915.
(13) Burczynski, M. E., Lin, H.-S., and Penning, T. M. (1999) Isoform-specific induction of a human aldo-keto reductase by polycyclic aromatic hydrocarbons (PAHs), electrophiles, and oxidative stress: Implications for the alternative pathway of PAH activation catalyzed by human dihydrodiol dehydrogenase. *Cancer Res. 59*, 607−614.
(14) Sachse, C., Smith, G., Wilkie, M. J. V., Barrett, J. H., Waxman, R., Sullivan, F., Forman, D., Bishop, D. T., Wolf, C. R., and the Colorectal Cancer Study Group (2002) A pharmacogenetic study to investigate the role of dietary carcinogens in the etiology of colorectal cancer. *Carcinogenesis 23*, 1839−1849.
(15) Talalay, P. (1989) Mechanisms of induction of enzymes that protect against chemical carcinogenesis. *Adv. Enzyme Regul. 28*, 237−250.
(16) Prestera, T., Holtzclaw, W. D., Zhang, Y., and Talalay, P. (1993) Chemical and molecular regulation of enzymes that detoxify carcinogens. *Proc. Natl. Acad. Sci. U.S.A. 90*, 2965−2969.
(17) Hayes, J. D., and Pulford, D. J. (1995) The glutathione S-transferase supergene family: Regulation of GST* and the contribution of the isoenzymes to cancer chemoprotection and drug resistance. *Crit. Rev. Biochem. Mol. Biol. 30*, 445−600.
(18) Cavalieri, E. L., and Rogan, E. G. (1995) Central role of radical cations in metabolic activation of polycyclic aromatic hydrocarbons. *Xenobiotica 25*, 677−688.
(19) Melendez-Colon, V. J., Luch, A., Seidel, A., and Baird, W. M. (1999) Cancer initiation by polycyclic aromatic hydrocarbons results from formation of stable DNA adducts rather than apurinic sites. *Carcinogenesis 20*, 1885−1891.
(20) Park, J.-H., Troxel, A. B., Harvey, R. G., and Penning, T. M. (2006) Polycyclic aromatic hydrocarbon (PAH) *o*-quinones produced by the aldo-keto-reductases (AKRs) generate abasic sites, oxidized pyrimidines, and 8-oxo-dGuo via reactive oxygen species. *Chem. Res. Toxicol. 19*, 719−728.
(21) Bolton, J. L., Trush, M. A., Penning, T. M., Dryhurst, G., and Monks, T. J. (2000) Role of quinones in toxicology. *Chem. Res. Toxicol. 13*, 135−160.
(22) Kim, K. B., and Lee, B. M. (1997) Oxidative stress to DNA, protein, and antioxidant enzymes (superoxide dismutase and catalase) in rats treated with benzo(*a*)pyrene. *Cancer Lett. 113*, 205−212.
(23) Canova, S., Degan, P., Peters, L. D., Livingstone, D. R., Voltan, R., and Venier, P. (1998) Tissue dose, DNA adduct, oxidative DNA damage and CYP1A-immunopositive proteins in mussels exposed to waterborne benzo[*a*]pyrene. *Mutat. Res. 399*, 17−30.
(24) Leadon, S. A. (1987) Production of thymine glycols in DNA by radiation and chemical carcinogens as detected by a monoclonal antibody. *Br. J. Cancer 55* (Suppl.), 113−117.
(25) Vaghef, H., Wisén A.-C., and Hellman, B. (1996) Demonstration of benzo(a)pyrene-induced DNA damage in mice by alkaline single cell gel electrophoresis: Evidence for strand breaks in liver but not in lymphocytes and bone marrow. *Pharmacol. Toxicol. 78*, 37−48.
(26) Seike, K., Murata, M., Oikawa, S., Hiraku, Y., Hirakawa, K., Mimura, and Kawanishi, S. (2003) Oxidative DNA damage induced by benz-[*a*]anthracene metabolites via redox cycles of quinone and unique non-quinone. *Chem. Res. Toxicol. 16*, 1470−1476.
(27) Miller, K. P., Chen, Y.-H., Hastings, V. L., Bral, C. M., and Ramos, K. S. (2000) Profiles of antioxidant/electrophile response element (ARE/EpRE) nuclear protein binding and *c*-Ha-ras transactivation in vascular smooth muscle cells treated with oxidative metabolites of benzo[*a*]pyrene. *Biochem. Pharmacol. 60*, 1285−1296.
(28) Chesis, P. L., Levin, D. E., Smith, M. T., Ernster, L., and Ames, B. N. (1984) Mutagenicity of quinones: Pathways of metabolic activation and detoxification. *Proc. Natl. Acad. Sci. U.S.A. 81*, 1696−1700.
(29) Flowers-Geary, L., Harvey, R. G., and Penning, T. M. (1993) Cytotoxicity of polycyclic hydrocarbon *o*-quinones in rat and human hepatoma cells. *Chem. Res. Toxicol. 6*, 252−260.
(30) Staal, Y. C. M., van Herwijnen, M. H. M., van Schooten, F. J., and van Delft, J. H. M. (2006) Modulation of gene expression and DNA adduct formation in HepG2 cells by polycyclic aromatic hydrocarbons with different carcinogenic potencies. *Carcinogenesis 27*, 646−655.
(31) Streitwieser, A., Jr., and Brown, S. M. (1988) Convenient preparation of 11*H*-benzo[*a*]fluorenone and 11*H*-benzo[*b*]fluorenone. *J. Org. Chem. 53*, 904−906.
(32) Fieser, L. F., and Joshel, L. M. (1940) 9-Methyl-3,4-benzofluorene. *J. Am. Chem. Soc. 62*, 957−958.
(33) Spijker, N. M., van den Braken-van Leersum, A. M., Lugtenburg, J., and Cornelisse, J. (1990) A very convenient synthesis of cyclopenta-[*cd*]pyrene. *J. Org. Chem. 55*, 756−758.
(34) Clar, E., and Mackay, C. C. (1972) Circobiphenyl and the attempted synthesis of 1:14, 3:4, 7:8, 10:11-tetrabenzoperopyrene. *Tetrahedron 28*, 6041−6047.
(35) Adachi, J., Mori, Y., Matsui, S., and Matsuda, T. (2004) Comparison of gene expression patterns between 2,3,7,8-tetrachlorodibenzo-*p*-dioxin and a natural arylhaydrocarbon receptor ligand, indirubin. *Toxicol. Sci. 80*, 161−169.
(36) Iwanari, M., Nakajima, M., Kizu, R., Hayakawa, K., and Yokoi, T. (2002) Induction of CYP1A1, CYP1A2, and CYP1B1 mRNAs by nitropolycyclic aromatic hydrocarbons in various human tissue-derived cells: Chemical-, cytochrome P450 isoform-, and cell-specific differences. *Arch. Toxicol. 76*, 287−298.
(37) Vakharia, D. D., Liu, N., Pause, R., Fasco, M., Bessette, E., Zhang, Q.-Y., and Kaminsky, L. S. (2001) Polycyclic aromatic hydrocarbon/metal mixtures: Effect on PAH induction of CYP1A1 in human HepG2 cells. *Drug Metab. Dispos. 29*, 999−1006.
(38) Bessette, E., Fasco, M. J., Pentecost, T., and Kaminsky, L. S. (2005) Mechanisms of arsenite-mediated decreases in benzo[*k*]fluoranthene-induced human cytochrome P4501A1 Levels in HepG2 cells. *Drug Metab. Dispos. 33*, 312−320.
(39) Jones, J. M., and Anderson, J. W. (1999) Relative potencies of PAHs and PCBs based on the response of human cells. *Environ. Toxicol. Pharmacol. 7*, 19−26.
(40) Jones, J. M., Anderson, J. W., and Tukey, R. H. (2000) Using the metabolism of PAHs in a human cell line to characteraize environmental samples. *Environ. Toxicol. Pharmacol. 8*, 119−126.
(41) Lekas, P., Tin, K. L., Lee, C., and Prokipcak, R. D. (2000) The human cytochrome P450 1A1 mRNA in rapidly degraded in HepG2 cells. *Arch. Biochem. Biophys. 384*, 311−318.
(42) Plakunov, I., Smolarek, T. A., Fischer, D. L., Wiley, J. C., Jr., and Baird, W. M. (1987) Separation by ion-pair high-performance liquid chromatography of the glucuronide, sulfate and glutathione conjugates formed from benzo[a]pyrene in cell cultures from rodents, fish and humans. *Carcinogenesis 8*, 59−66.
(43) Nesnow, S., Ross, J. A., Mass, M. J., and Stoner, G. D. (1998) Mechanistic relationships between DNA adducts, oncogene mutations, and lung tumorigenesis in strain A mice. *Exp. Lung Res. 24*, 395−405.
(44) Rice, J. E., Coleman, D. T., Hosted, T. J., Jr., LaVoie, E. J., and Wiley, J. C., Jr. (1985) Identification of mutagenic metabolites of indeno-[1,2,3-*cd*]pyrene formed *in vitro* with rat liver enzymes. *Cancer Res. 45*, 5421−5425.
(45) Monks, T. J., Hanzlik, R. P., Cohen, G. M., Ross, D., and Graham, D. G. (1992) Quinone chemistry and toxicity. *Toxicol. Appl. Pharmacol. 112*, 2−16.
(46) Rowe, J. D., Nieves, E., and Listowsky, I. (1997) Subunit diversity and tissue distribution of human glutathione S-transferase: Interpretations based on electrospray ionization-MS and peptide sequence-specific antisera. *Biochem. J. 325*, 481−486.
(47) Aninat, C., Piton, A., Glaise, D., Charpentier, T. L., Langouët, Morel, F., Guguen-Guillouzo, C., and Guillouzo, A. (2006) Expression of cytochromes P450, conjugating enzymes and nuclear receptors in human hepatoma HepaRG cells. *Drug Metab. Dispos. 34*, 75−83.
(48) Sundberg, K., Dreij, K., Seidel, A., and Jernström, B. (2002) Glutathione conjugation and DNA adduct formation of dibenzo[*a,l*]-pyrene and benzo[*a*]pyrene diol epoxides in V79 cells stably expressing different human glutathione transferases. *Chem. Res. Toxicol. 15*, 170−179.
(49) Zhao, W., and Ramos, K. S. (1998) Cytotoxic response profiles of cultured rat hepatocytes to selected aromatic hydrocarbons. *Toxicol. in Vitro 12*, 175−182.

TX060197U

Available online at www.sciencedirect.com
ScienceDirect
Mutation Research 626 (2007) 15–25
Genetic Toxicology and Environmental Mutagenesis
www.elsevier.com/locate/gentox
Community address: www.elsevier.com/locate/mutres

Combined genotoxic effects of radiation and a tobacco-specific nitrosamine in the lung of *gpt* delta transgenic mice

Megumi Ikeda [a,b], Ken-ichi Masumura [a], Yasuteru Sakamoto [a], Bing Wang [c], Mitsuru Nenoi [c], Keiko Sakuma [b], Isamu Hayata [c], Takehiko Nohmi [a,*]

[a] *Division of Genetics and Mutagenesis, National Institute of Health Sciences, 1-18-1 Kamiyoga, Setagaya-ku, Tokyo 158-8501, Japan*
[b] *Graduate School of Nutrition and Health Sciences, Kagawa Nutrition University, 3-9-21 Chiyoda, Sakado-shi, Saitama 350-0288, Japan*
[c] *Radiation Effect Mechanisms Research Group, Research Center of Radiation Protection, National Institute of Radiological Sciences, 4-9-1 Anagawa, Inage-ku, Chiba-shi, Chiba 263-8555, Japan*

Received 22 May 2006; received in revised form 25 July 2006; accepted 31 July 2006
Available online 7 September 2006

Abstract

It is important to evaluate the health effects of low-dose-rate or low-dose radiation in combination with chemicals as humans are exposed to a variety of chemical agents. Here, we examined combined genotoxic effects of low-dose-rate radiation and 4-(methylnitrosamino)-1-(3-pyridyl)-1-butanone (NNK), the most carcinogenic tobacco-specific nitrosamine, in the lung of *gpt* delta transgenic mice. In this mouse model, base substitutions and deletions can be separately analyzed by *gpt* and Spi$^-$ selections, respectively. Female *gpt* delta mice were either treated with γ-irradiation alone at a dose rate of 0.5, 1.0 or 1.5 mGy/h for 22 h/day for 31 days or combined with NNK treatments at a dose of 2 mg/mouse/day, i.p. for four consecutive days in the middle course of irradiation. In the *gpt* selection, the NNK treatments enhanced the mutation frequencies (MFs) significantly, but no obvious combined effects of γ-irradiation were observable at any given radiation dose. In contrast, NNK treatments appeared to suppress the Spi$^-$ large deletions. In the Spi$^-$ selection, the MFs of deletions more than 1 kb in size increased in a dose-dependent manner. When NNK treatments were combined, the dose–response curve became bell-shaped where the MF at the highest radiation dose decreased substantially. These results suggest that NNK treatments may elicit an adaptive response that eliminates cells bearing radiation-induced double-strand breaks in DNA. Possible mechanisms underlying the combined genotoxicity of radiation and NNK are discussed, and the importance of evaluation of combined genotoxicity of more than one agent is emphasized.

Keywords: Combined genotoxic effects; Radiation; NNK; Lung cancer; *gpt* delta mice; Deletion

1. Introduction

Environmental factors play important roles in the etiology of human cancer [1]. Of various environmental hazardous compounds, cigarette smoke is the most causative factor associated with the increase in cancer risk in humans. Tobacco smoking plays a major role in the etiology of lung, oral cavity and esophageal cancers, and a variety of chronic degenerative diseases [2]. Although cigarette smoke is a mixture of about 4000 chemicals including more than 60 known human carcinogens, 4-(methylnitrosamino)-1-(3-pyridyl)-1-butanone (nicotine-derived nitrosamino ketone, NNK) is the most carcinogenic tobacco-specific nitrosamine [3,4]. NNK induces lung tumors in mice,

* Corresponding author. Tel.: +81 3 3700 9873; fax: +81 3 3707 6950.
E-mail address: nohmi@nihs.go.jp (T. Nohmi).

1383-5718/$ – see front matter © 2006 Elsevier B.V. All rights reserved.
doi:10.1016/j.mrgentox.2006.07.003

rats and hamsters, and International Agency for Research on Cancer has concluded that exposure to NNK and NNN (*N'*-nitrosonornicotine) is carcinogenic to humans [5]. NNK is metabolically activated by CYP (P-450) enzymes in the lung and generates O^6-methylguanine in DNA, which leads to G:C to A:T mutations, and the subsequent activation of Ki-*ras* proto-oncogene, an initiation of tumor development [6,7].

Radiation, on the other hand, is one of the most causative physical factors that induce human cancer. Radiation induces double-strand breaks (DSBs) in DNA, which lead to chromosome aberrations and cell deaths, and generates a variety of oxidative DNA damage [8]. Because of the genotoxicity, radiation at high doses clearly induces various tumors in humans [9]. Even at low doses, residential exposure to radioactive radon and its decay products may account for about 10% of all lung cancer deaths in the United States and about 20% of the lung cancer cases in Sweden [10,11].

Since humans are exposed to a variety of chemical and physical agents that may induce cancer, these factors may interact with each other and the action of one agent may be influenced by exposure to another agent [12]. The risk from combined exposure to more than one agent may be substantially higher or lower than predicted from the sum of the individual agents. In fact, low-dose radiation can induce an adaptive response, causing rodent or human cells to become resistant to genotoxic damage by subsequent higher doses of radiation [13]. Pre-exposure to alkylating agents at low doses induces another adaptive response that provides mechanisms by which the exposed bacterial cells can tolerate the higher challenging doses of genotoxic agents [14]. In addition, mitomycin C, bleomycin, hydrogen peroxide, metals and quercetin may also induce an adaptive response [15].

To explore the mechanisms underlying the interactive effects of chemical and physical agents on carcinogenesis, we examined the combined genotoxic effects of NNK and γ-irradiation in the lung of *gpt* delta transgenic mice [16]. In this mouse model, point mutations and deletions are separately analyzable by *gpt* and Spi^- selections, respectively [17]. Point mutations such as base substitutions are induced by a number of chemical carcinogens including NNK [18]. Spi^- selection detects deletions in size between 1 bp and 10 kb [19]. Deletions in size more than 1 kb, which we call large deletions in this study, are efficiently induced by γ-ray, X-ray and carbon-ion irradiation [20], and are thought to be generated by non-homologous end joining (NHEJ) of DSBs in DNA [21].

We report here that low-dose-rate γ-irradiation enhanced the mutation frequencies (MFs) of the large deletions in the lung of *gpt* delta mice in a dose-dependent manner. When combined with NNK treatments, however, the MF at the highest radiation dose, i.e., 1.02 Gy, was reduced by more than 50%, suggesting that NNK treatments may induce an adaptive response against radiation-induced deletion mutations. We discuss possible mechanisms of the adaptive response and emphasize the importance of the risk assessment of combined genotoxic effects of radiation and chemicals in vivo.

2. Materials and methods

2.1. Treatment of mice

gpt delta C57BL/6J transgenic mice were maintained in the conventional animal facility of National Institute of Radiological Sciences, Chiba, Japan, according to the institutional animal care guidelines. They were housed in autoclaved aluminum cages with sterile wood chips for bedding and given free access to standard laboratory chow (MB-1, Funabashi Farm Co., Japan) and acidified water under controlled lighting (12 h light/dark cycle). Seven-week-old female *gpt* delta mice were divided to eight groups each consisting of six mice. Three groups were γ-irradiated at a dose rate of 0.5, 1.0 or 1.5 mGy/h for 22 h/day for 2 weeks (Fig. 1). After the irradiation, three groups of mice were treated with a single i.p. injection of NNK (Toronto Research Chemicals, Toronto, Canada) dissolved in saline at a daily dose of 2 mg/mouse for four consecutive days. The irradiation continued during the 4-day treatments, and the mice were kept in the cage for another 2 weeks with irradiation. Three control groups were γ-irradiated as described but received saline instead of NNK. The whole irradiation period was 31 days, and the total estimated doses were 0.34, 0.68 and 1.02 Gy, respectively. Another control group of mice was treated with NNK as described but without γ-irradiation. The third control was kept in the cage for 31 days without γ-irradiation or NNK treatments. The source of radiation was ^{137}Cs, and the dose rate was estimated by a fluorescent glass dosimeter. The non-irradiated control groups were placed behind a concrete wall of 1 m thickness. The mice were sacrificed by cervical vertebral dislocation. The liver and lung were removed, placed immediately in liquid nitrogen, and stored at −80 °C until analysis.

2.2. DNA isolation and in vitro packaging of DNA

High-molecular-weight genomic DNA was extracted from the lung and the liver using the RecoverEase DNA Isolation Kit (Stratagene, La Jolla, CA). Lambda EG10 phages were rescued using Transpack Packaging Extract (Stratagene, La Jolla, CA).

2.3. gpt mutation assay

The *gpt* mutagenesis assay was performed according to previously described methods [17]. Briefly, *Escherichia coli*

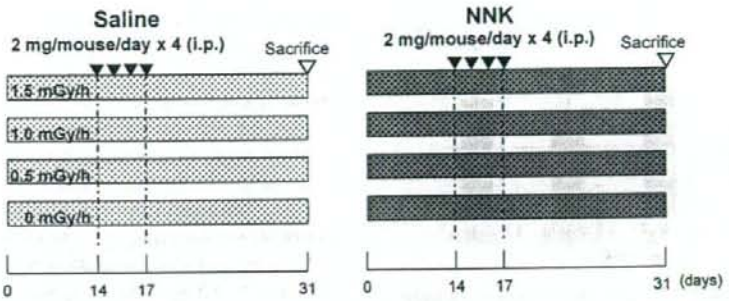

Fig. 1. An experimental design to examine the combined genotoxicity of γ-irradiation and NNK treatments in the lung of mice. Female 7-week-old *gpt* delta mice were divided into eight groups each composed of six mice. Three groups of mice were irradiated at a dose rate of 0.5, 1.0 or 1.5 mGy/h for 22 h/day for 14 days and treated with NNK at a daily dose of 2 mg/mouse for four consecutive days. The irradiation continued during the NNK treatments and the following 14 days before sacrifice. The total radiation doses were 0.34, 0.68 and 1.02 Gy, respectively. Control three groups of mice were γ-irradiated but without NNK treatments. Another control group was treated with NNK but without γ-irradiation. The third control was kept in the cage for 31 days without γ-irradiation or NNK treatments. Transgene λEG10 DNA was rescued from the lung of mice, and the base substitutions and deletions were analyzed by *gpt* and Spi⁻ selection, respectively.

YG6020 expressing Cre recombinase was infected with the rescued phage. The bacteria were then spread onto M9 salts plates containing chloramphenicol (Cm) and 6-thioguanien (6-TG), and incubated for 72 h at 37 °C for selection for the colonies harboring a plasmid carrying the Cm acetyltransferase (*cat*) gene and a mutated *gpt* gene. The 6-TG-resistant colonies were streaked again onto the same selection plates for confirmation of the resistant phenotype. All the confirmed *gpt* mutants recovered from the lung were sequenced and the identical mutations from the same mouse counted one mutant. The *gpt* MFs in the lung were calculated by dividing the number of the *gpt* mutants after sequencing by the number of rescued plasmids, which was estimated from the number of colonies on plates containing Cm but without 6-TG. Since no *gpt* mutants recovered from the liver were sequenced, the MFs in the liver were calculated by dividing the number of confirmed 6-TG-resistant colonies by the number of rescued plasmids.

2.4. PCR and DNA sequencing analysis of 6-TG-resistant mutants

A 739 bp DNA fragment containing the *gpt* gene was amplified by polymerase chain reaction (PCR) using primers 1 and 2 [17]. The reaction mixture contained 5 pmol of each primer and 200 mM of each dNTP. PCR amplification was carried out using Ex Taq DNA polymerase (Takara Bio, Shiga, Japan) and performed with a Model PTC-200 Thermal Cycler (MJ Research, Waltham, MA). PCR products were analyzed by agarose gel electrophoresis to determine the amount of the products. DNA sequencing of the *gpt* gene was performed with BigDye™ Terminator Cycle Sequencing Kit (Applied Biosystems, Foster City, CA) using sequencing primer gptA2 (5′-TCTCGCGCAACCTATTTTCCC-3′). The sequencing reaction products were analyzed on an Applied Biosystems model 310 genetic analyzer (Applied Biosystems, Foster City, CA).

2.5. Spi⁻ mutation assay

The Spi⁻ assay was performed as described previously [17]. The lysates of Spi⁻ mutants were obtained by infection of *E. coli* LE392 with the recovered Spi⁻ mutants. The lysates were used as templates for PCR analysis to determine the deleted regions. Sequence changes in the *gam* and *redAB* genes, and the outside of the *gam/redAB* genes were identified by DNA sequencing analysis [22]. The appropriate primers for DNA sequencing were selected based on the results of PCR analysis. The entire sequence of λEG10 is available at http://dgm2alpha.nhis.go.jp.

2.6. Statistical analysis

All data are expressed as mean ± standard deviations of the MFs of six mice for lung and those of four mice for liver. Differences between groups were tested for statistical significance using a Student's *t*-test. A p value less than 0.05 denoted the presence of a statistically significant difference.

3. Result

3.1. gpt MFs in the lung of NNK-treated and γ-irradiated gpt delta mice

We measured the *gpt* MFs in the lung of *gpt* delta mice untreated or treated with NNK in the absence or the presence of γ-irradiation (Fig. 2). NNK treatments significantly enhanced the MFs over the control groups. The mean MFs ($\times 10^{-6}$) of NNK-treated versus saline-treated groups were 14.3 ± 6.9 versus 4.2 ± 4.0, 20.7 ± 5.1 versus 4.7 ± 3.0, 15.2 ± 7.3 versus 2.0 ± 2.1 and 17.2 ± 7.9 versus 2.7 ± 1.4 at the dose rates of 0, 0.5, 1.0 and 1.5 mGy/h, respectively. The γ-irradiation

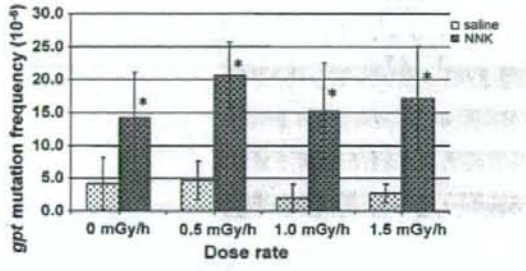

Fig. 2. *gpt* MFs in the lung of mice untreated or treated with NNK in the absence or the presence of γ-irradiation. An asterisk (*) denotes $p < 0.05$ ($n = 6$) in a Student's *t*-test of MF of NNK-treated vs. the corresponding untreated mice. Vertical bars show the standard deviations with mice as the unit of comparison.

alone, i.e., the saline-treated group, did not enhance the *gpt* MF under the conditions. Hence, the increases in MFs are due to NNK treatments. Although the individual MFs slightly varied, there was no significant difference among the four MFs of the NNK-treated groups. Thus, we suggested that the irradiation did not modify the genotoxicity of NNK in the lung of mice.

To confirm the results in the lung, we analyzed the *gpt* MFs in the liver of the NNK-treated and saline-treated groups. The mean MFs ($\times 10^{-6}$) of NNK-treated versus saline-treated groups were 134 ± 48 versus 8.1 ± 3.8, 105 ± 31 versus 8.7 ± 3.5, 101 ± 18 versus 8.0 ± 4.2 and 128 ± 76 versus 6.8 ± 0.6 at the dose rates of 0, 0.5, 1.0 and 1.5 mGy/h, respectively. Although NNK treatments induced mutations much more strongly in the liver than in the lung, there were no significant modulating effects of radiation on the NNK-induced mutations in the liver.

The irradiation might modulate specific types of mutations without affecting the total *gpt* MFs. To examine the possibility, we determined the mutation spectra of the *gpt* gene in the lung and examined whether the radiation affected specific types of mutations (Table 1). NNK treatments induced G:C to A:T, G:C to T:A, A:T to T:A and A:T to C:G mutations. In particular, A:T to T:A mutations were induced more than 20-fold by NNK treatments. We observed, however, no remarkable variations of mutation spectra associated with the dose rates of combined radiation. Thus, we concluded that the irradiation did not enhance or suppress the base substitutions induced by NNK in the lung of *gpt* delta mice significantly.

3.2. Spi⁻ MFs in the lung of NNK-treated and γ-irradiated gpt delta mice

Next, we measured the Spi⁻ MFs in the lung of *gpt* delta mice untreated or treated with NNK in the absence or the presence of γ-irradiation. The mean Spi⁻ MFs ($\times 10^{-6}$) of NNK-treated versus saline-treated groups were 5.15 ± 2.34 versus 4.11 ± 0.98, 5.47 ± 1.98 versus 5.06 ± 3.50, 5.36 ± 1.56 versus 4.09 ± 0.80 and 5.39 ± 2.56 versus 4.65 ± 1.78 at the dose rates of 0, 0.5, 1.0 and 1.5 mGy/h, respectively. These results suggest that neither NNK treatments nor the irradiation enhanced the Spi⁻ MFs in the lung significantly.

To investigate the combined effects of NNK and γ-irradiation on specific types of deletion mutations, we identified all the Spi⁻ mutations by DNA sequencing analysis (Table 2). Of various classes of deletions observed, only the MFs of large deletions in the size of more 1 kb increased in a dose-dependent manner in the saline-treated group. To examine the dose–response in more detail, we determined the MFs of the large deletions

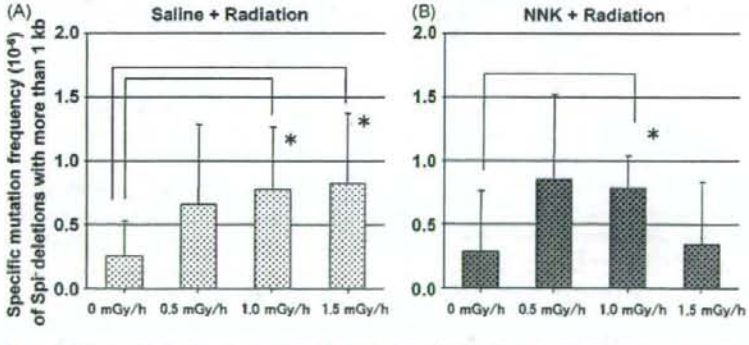

Fig. 3. Specific MF of large deletions with the size of more than 1 kb in the lung of unirradiated or γ-irradiated mice. The mice were not treated (A) or treated with NNK (B). An asterisk (*) denotes $p < 0.05$ ($n = 5$) in a Student's *t*-test of MF of γ-irradiated vs. the corresponding unirradiated mice. Vertical bars show the standard deviations with mice as the unit of comparison.

Table 1
gpt mutation spectra in the lung of NNK-treated and γ-irradiated *gpt* delta mice

Treatment: saline	0 mGy/h			0.5 mGy/h			1.0 mGy/h			1.5 mGy/h		
	No.	MF ($\times 10^{-6}$)	%	No.	MF ($\times 10^{-6}$)	%	No.	MF ($\times 10^{-6}$)	%	No.	MF ($\times 10^{-6}$)	%
Base substitution												
Transition												
G:C → A:T	15(6)	1.81	43	12(6)	1.76	38	5(2)	0.61	29	8(4)	0.81	30
A:T → G:C	2	0.24	6	4	0.59	13	1	0.12	6	2	0.20	7
Transversion												
G:C → T:A	1	0.12	3	5(2)	0.73	16	1	0.12	6	6(1)	0.61	22
G:C → C:G	1	0.12	3	0	0.00	0	0	0.00	0	2(2)	0.20	7
A:T → T:A	1	0.12	3	1	0.15	3	1	0.12	6	1	0.10	4
A:T → C:G	3	0.36	9	1	0.15	3	1	0.12	6	1	0.10	4
Deletion	8	0.97	23	6	0.88	19	7	0.85	41	6	0.61	22
−1 bp	3			2			5			3		
>2 bp	5			4			2			3		
Insertion	3	0.36	9	3	0.44	9	1	0.12	6	1	0.10	4
Others	1	0.12	3	0	0.00	0	0	0.00	0	0	0.00	0
	35	4.23	100	32	4.69	100	17	2.06	100	27	2.73	100
Treatment: NNK	0 mGy/h			0.5 mGy/h			1.0 mGy/h			1.5 mGy/h		
	No.	MF ($\times 10^{-6}$)	%	No.	MF ($\times 10^{-6}$)	%	No.	MF ($\times 10^{-6}$)	%	No.	MF ($\times 10^{-6}$)	%
Base substitution												
Transition												
G:C → A:T	24(2)	5.11	36	45(8)	8.02	39	32(5)	5.85	39	54(6)	8.51	50
A:T → G:C	0	0.00	0	7	1.25	6	6	1.10	7	2	0.32	2
Transversion												
G:C → T:A	9(2)	1.92	13	10(1)	1.78	9	7(1)	1.28	8	7(1)	1.10	6
G:C → C:G	0	0.00	0	2	0.36	2	0	0.00	0	3	0.47	3
A:T → T:A	13	2.77	19	26	4.64	22	17	3.11	21	17(1)	2.68	16
A:T → C:G	15	3.19	22	12	2.14	10	8	1.46	10	12(1)	1.89	11
Deletion	5	1.06	8	12	2.14	10	9	1.65	11	12	1.89	11
−1 bp	5			6			4			5		
>2 bp	0			6			5			7		
Insertion	1	0.21	2	0	0.00	0	4	0.73	5	1	0.16	1
Others	0	0.00	0	2	0.36	2	0	0.00	0	1	0.16	1
	67	14.26	100	116	20.68	100	83	15.18	100	109	17.18	100

No. stands for the number of mutations.

of each mouse and calculated the mean MF and standard derivations. The mean MFs ($\times 10^{-6}$) and standard derivations were 0.25 ± 0.28, 0.66 ± 0.63, 0.77 ± 0.49 and 0.82 ± 0.55 at the dose rates of 0, 0.5, 1.0 and 1.5 mGy/h, respectively (Fig. 3A). The values at 1.0 and 1.5 mGy/h were about three-fold higher than the value at 0 mGy/h, and the differences were statistically significant ($p = 0.04$). In contrast, the dose–response curve of large deletions in NNK-treated group was a bell shaped (Fig. 3B). The mean MFs ($\times 10^{-6}$) and standard derivations of large deletions in the NNK-treated group were 0.29 ± 0.47, 0.85 ± 0.66, 0.78 ± 0.26 and 0.35 ± 0.48 at the dose rates of 0, 0.5, 1.0 and 1.5 mGy/h, respectively. It should be noted that the

Table 2
Spi⁻ mutation spectra in the lung of NNK-treated and γ- irradiated *gpt* delta mice

Treatment: saline	0 mGy/h			0.5 mGy/h			1.0 mGy/h			1.5 mGy/h		
	No.	MF ($\times 10^{-6}$)	%	No.	MF ($\times 10^{-6}$)	%	No.	MF ($\times 10^{-6}$)	%	No.	MF ($\times 10^{-6}$)	%
1 bp deletion												
Simple												
Guanine	9	0.49	12	7	0.59	12	5	0.34	8	4	0.30	7
Adenine	4	0.22	5	0	0.00	0	2	0.14	3	1	0.08	2
In run												
Guanine	13	0.71	17	15	1.27	25	12	0.82	20	13	0.99	21
Adenine	31	1.70	41	19	1.60	32	22	1.50	37	25	1.91	41
With b.s.	0	0.00	0	0	0.00	0	0	0.00	0	0	0.00	0
>2 bp deletion	15	0.82	20	17	1.43	28	17	1.16	28	13	0.99	21
2 bp ~ 1 kb	2	0.11	3	7	0.59	12	3	0.20	5	1	0.08	2
>1 kb	5	*0.27*	7	7	*0.59*	12	11	*0.75*	18	10	*0.76*	16
Complex	8	0.44	11	3	0.25	5	3	0.20	5	2	0.15	3
Insertion	3	0.16	4	2	0.17	3	2	0.14	2	5	0.38	8
	75	4.11	100	60	5.06	100	60	4.09	100	61	4.65	100
Treatment: NNK	0 mGy/h			0.5 mGy/h			1.0 mGy/h			1.5 mGy/h		
	No.	MF ($\times 10^{-6}$)	%	No.	MF ($\times 10^{-6}$)	%	No.	MF ($\times 10^{-6}$)	%	No.	MF ($\times 10^{-6}$)	%
1 bp deletion												
Simple												
Guanine	5	0.61	12	4	0.46	8	4	0.50	9	4	0.48	9
Adenine	3	0.37	7	0	0.00	0	4	0.50	9	1	0.12	2
In run												
Guanine	9	1.10	21	19	2.17	40	9	1.12	21	14	1.68	31
Adenine	12	1.47	29	10	1.14	21	9	1.12	21	15	1.80	33
With b.s.	0	0.00	0	0	0.00	0	2	0.25	5	0	0.00	0
>2 bp deletion	12	1.47	29	10	1.14	21	11	1.37	26	11	1.32	24
2 bp ~ 1 kb	6	0.74	14	2	0.23	4	3	0.37	7	7	0.84	16
>1 kb	2	*0.25*	5	7	*0.80*	15	7	*0.87*	16	2	*0.24*	4
Complex	4	0.49	10	1	0.11	2	1	0.12	2	2	0.24	4
Insertion	1	0.12	2	5	0.57	10	4	0.50	9	0	0.00	0
	42	5.15	100	48	5.47	100	43	5.36	100	45	5.39	100

No. stands for the number of mutations. Specific MFs of large deletions more than 1 kb in size are italicised.

MF at 1.0 mGy/h (0.78×10^{-6}) was about three-fold higher than that of 0 mGy/h ($p = 0.04$) but the MF at 1.5 mGy/h (0.35×10^{-6}) was very similar to that of 0 mGy/h (0.29×10^{-6}). The p values of the differences of MFs between saline-treated and NNK-treated groups at dose rates of 0, 0.5, 1.0 and 1.5 mGy/h were 0.44, 0.32, 0.48 and 0.09, respectively. From the results, we suggested that NNK treatments suppressed the induc-

Fig. 4. Molecular nature of large deletions recovered from the lung of *gpt* delta mice untreated or treated with NNK in the absence or the presence of γ-irradiation. Horizontal bars represent the deleted regions of mutants. Most of the mutants lack the entire *gam* gene and part of the *redAB* genes, but some lack the *gam* gene and the upstream region. The *gam* and *redAB* genes make an operon and the transcription starts from the upstream of the *gam* gene. Short homologous sequences in the junctions of the mutants are underlined. Underlined sequences, i.e., T or CTTA, in the middle of two sequences are inserted sequences in the junctions.

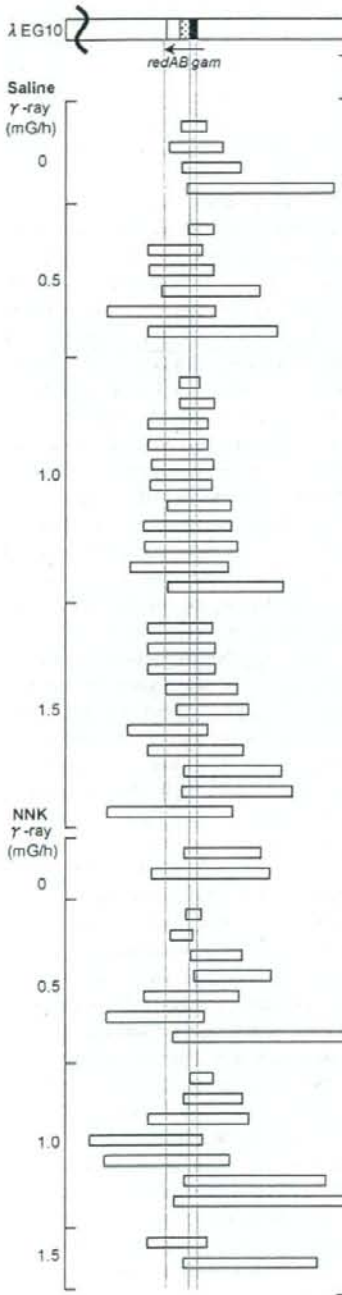

Delesion size (bp)	Sequence of the junction of deletion		No.of mutant	Mouse I.D.
- 1242	TGAATGGTTCGCGGCGGC	GTGTTTGTGCATCCATCT	2	2,34
- 2912	AGAGCAGGCGGTACGCAT	TAATCCTTAACTTTGCCC	1	34
- 3393	GGTAAATCCGGCATGTAC	AGCCAGGGGATCTCTCCC	1	34
- 7626	CAGCCAGCGTTGCGAGTG	CGGTTGCTTTATGCATGG	1	3
- 1608	GCTATCACGTTGTGAACT	TCGGATTTAGTGCGCTTT	2	9,11
- 2912	AGAGCAGGCGGTACGCAT	TAATCCTTAACTTTGCCC	1	9
- 3650	ACTGTTGGTTAATACGCT	AAAGCTCCAAGCTCAACA	1	41
- 5339	GATGCGGCTAACGTATGA	TGCCTTTGCGGCTTGTAA	1	11
- 5582 + 1	CGCCTGTCTCTGCCTAAT	T ATACTCTCTAATCTTGGC	1	10
- 6789	CATCCTGAACCCATTGAC	ACCACAGCGTGATGGGCT	1	10
- 1164	ATGGTTCGCGGCGGCATT	TTGCGCTTACCCCAACCA	1	50
- 1922	CACTGAATCATGGCTTTA	AGAAGCAATAACCCGCAG	1	50
- 3219	TTCTATTTCTGATGCTGA	GTATCACACACCCCAAAG	1	19
- 3326	TGATGTATTGCTGGTTTC	CTGGTTTTGCGCTTACCC	1	19
- 3360	GATTTCAGAATTAGCCTG	GGGTATCATGTAGCCGCT	1	49
- 3473	GCGGCGTTTGATGTATTG	TGTGGCAGTTGTAGTCCT	1	19
- 3966	TAACTTCCGGAGCCACAC	GAAGACGCGATCTCGCTC	1	17
- 4716	TCCTTTGATGCGAATGCC	GCATAATTACTCCTGATA	1	18
- 5053	AATTCATGGAAAAGGTCT	GCGTAAACTCCGCTGTCA	1	50
- 5244	GTATCAGCAATGTTTATG	GTAGCTTGGCTTCTACCT	1	17
- 6140	ATCGGGGATTCAGTAACA	CGCCTTCTGTCACCACCA	1	10
- 3645	GGTCTGCGTCAAATCCCC	GGTTATCTGTATGTTTTT	1	27
- 3833	AATCGATGGTGTTACCAA	AACCCGGCGCTGAGGCCG	1	57
- 3879	TTGCTGGTTTCTTTCCCG	CTGAGGCCGGGTTATTCT	1	27
- 4014	TTTTCGATGAACTCCGGC	CTTACCGGGTTATCCCCA	1	26
- 4035	CTTCCCAGCCAGCGTTGC	CCTGCACCAGCGTGGTAA	1	27
- 4416	TAAAATAAATCCCCGCGA	TTGGCACATTGGCAGCTA	1	27
- 5194	ATAACTCTGTTGAATGGC	ATATGATGACAATGTCGC	1	58
- 5366	TAACGCAGATCGGATGAT	CCGCCAGTGGCGCACTAT	1	58
- 5905	GGAACAGAGCGGCAATAA	CTGCCTGATTAGCGGCGA	1	25
- 6629	CCGCAATTTCTTTTGTGG	CCTTCAACAAACAAAAAA	1	26
- 4283	TGATGATGCGGGACCAGC	GACCACGCCTTTGGGGCG	1	38
- 6283	TTGCCAGGCTTAAATGAG	ATCTAAGGCCGTCACCTG	1	5
- 1035	ATCACCTTTAAATGCCGT	AACCCCCCGCGATTGGCA	1	15
- 1315	CAGTGCTTTAGCGTTAAC	ATAGCTGTGAAAATATCG	1	45
- 2724	TGCTGGCCCCGTGGCGTT	CTCCAGCCCCTATCCCCC	1	45
- 4318	CCTTTTTCCATGTCGTCT	CAGCGGGTACGGTTGGCG	1	13
- 5146	CGAGAAGATGTTGAGCAA	TCTGCCAGTTCTGCCTCT	1	15
- 5273	GCTGACGCCGCCTTGCCC	CCCGCGATTGGCACATTG	1	14
- 9265	TGTGCCACGCATCATCCC	ATGGATGCAGCCTCCAGA	1	15
- 1373	GTGAGCAATGGTTTCAAC	TGGCGATAGTGGGTATCA	1	23
- 3466	AGGATTCATTGTCCTGCT	GTTCGCCACCCAACCCGC	1	53
- 5445	GTTTAACATGCCGATTGC	AGCGCGCGTAATCCGGCG	1	54
- 5974	ATCCGGATGAAGCCGCTT	GCAATGTATGTCGTTTCA	1	21
- 6666 + 4	GCCGTAAGTCTTGATCTC	CTTA CCTCATCAGTGGCTCTAT	1	22
- 7430	TTTGAATGGTTCGCGGCG	CGTAGCGGTGGAAGTGGC	1	21
- 9265	TTGTGCCACGCATCATCC	ATGGATGCAGCCTCCAGA	1	21
- 3219	GTAATAGCGATGCGTAAT	AGGAAAACAGGAAAGGGG	1	61
- 7081	TCAGCCAGCTTCCCAGCC	GGTGGAAGTGGCGATGAA	1	30

tion of large deletions at a dose rate of 1.5 mGy/h of γ-irradiation.

To further characterize the large deletions induced by the irradiation, we identified the size and junctions of all the 51 deletion mutants (Fig. 4). The size of deletions distributed from 1035 to 9265 bp. About half of the mutants had short homologous sequences up to 11 bp in the junctions while another half had no such short homologous sequences. Two mutants had 1 or 4 bp insertions in the junctions. There was no hot spot of the junctions so that only 2 out of 51 deletions were identified in two mice. There were no obvious differences between large deletions induced by radiation alone and those induced by radiation plus NNK treatments. These results suggest that radiation-induced DSBs in DNA caused large deletions either in the absence or the presence of NNK treatments.

4. Discussion

Humans are exposed to a variety of exogenous and endogenous genotoxic agents. Thus, biological effects of radiation at low doses or low-dose-rate should be evaluated in combination with chemical exposure [12]. In fact, survey of chromosome aberrations in habitats in high-background radiation area in China indicates that cigarette smoking has stronger effects on induction of chromosome aberrations than has the elevated level of natural radiation [23]. Epidemiological studies on underground mineworkers exposed to high levels of radon or plutonium suggest the complexity of interactions between radiation and cigarette smoke in induction of lung tumors [24,25]. Hence, it is important to understand the fundamental mechanisms underlying the interactive genotoxicity and carcinogenicity of cigarette smoking and radiation for the risk assessment on human health.

To elucidate the mechanisms involved, we examined the combined genotoxicity of low-dose-rate γ-irradiation and a tobacco-specific nitrosamine NNK in the lung of *gpt* delta mice. In this study, we focused on whether γ-irradiation would modulate NNK-induced base substitutions and whether NNK treatments would modulate radiation-induced deletions. The mice were irradiated at dose rates of 0.5, 1.0 and 1.5 mGy/h for 22 h for 2 weeks and treated with NNK, i.e., 2 mg/mouse/day for four consecutive days, with irradiation (Fig. 1). The mice were irradiated at the same dose rates for another 2 weeks before sacrifice. Base substitutions and deletions in the lung detected by *gpt* and Spi$^-$ selection, respectively, were analyzed at the molecular levels. We chose the dose rates, i.e., 0.5, 1.0 and 1.5 mGy/h of γ-ray, since Sakai et al. [26] report the suppression of carcinogenicity of 3-methylchoranthrene in ICR female mice by chronic low-dose-rate irradiation of γ-ray at 0.95 mGy/h. According to the report, there is an optimum dose rate of about 1 mGy/h to observe the suppressive effects, and the higher or lower dose rates fail to suppress the tumor induction.

In the present study, NNK treatments significantly enhanced the *gpt* MF (Fig. 2). We observed, however, no modulating effects, i.e., enhancement or suppression, of γ-irradiation at any given dose rate, on the NNK-induced mutations (Fig. 2). This conclusion holds true even when we analyzed the detailed mutation spectra (Table 1). NNK treatments induced similar pattern of base substitutions, i.e., G:C to A:T, G:C to T:A, A:T to T:A and A:T to C:G regardless of the dose rates of combined radiation. In contrast, we observed a suppressive effect of NNK treatments on the radiation-induced deletions. γ-Irradiation enhanced the MF of large deletions in the size of more than 1 kb in a dose-dependent manner (Fig. 3A and Table 2). When combined with NNK treatments, however, the dose–response curve became bell-shaped and the MF at the highest dose rate, i.e., 1.5 mGy/h, was reduced by more than 50% (Fig. 3B and Table 2). The total radiation dose at the highest dose rate was 1.02 Gy. The size of the large deletions was between about 1 and 9 kb, and about half of the large deletions had short homologous sequences in the junctions while other did not (Fig. 4). These features are similar to those of large deletions induced by high dose irradiation with heavy ion, X-ray and γ-ray [20]. Thus, we suggest that NNK induced an adaptive response that eliminated the cells bearing radiation-induced DSBs in DNA.

Previous studies show that low-dose radiation can induce an adaptive response, which causes cells to become resistant to damage by subsequent high doses of radiation [13,27]. Although the exact mechanisms of the adaptive response are not well understood, it is assumed that some proteins are induced by low-dose radiation and they recognize and remove the cells bearing DSB in DNA. Tucker et al. [28] report that the frequency of *Dlb-1* mutations in the small intestine in female F1 mice obtained by crossing SWR/J and C57BL/6 increases along with the total radiation doses of γ-ray, but it saturates and slightly decreases at high doses, i.e., 2–3 Gy (55 mGy/day × 42 or 63 days). Interestingly, our results also suggest that the MFs of the large deletions saturated slightly at the highest dose of 1.02 Gy (Fig. 3A). Thus the adaptive response might be induced slightly at the highest radiation dose even without NNK treatments. Nevertheless, concomitant NNK treatments much clearly suppressed the occurrence of large dele-

tions at the highest radiation dose. We speculate that NNK treatments plus radiation at the highest dose may induce p53-dependent apoptosis, which eliminates the cells bearing radiation-induced DSBs in DNA [29]. The involvement of p53 in the maintenance of genome stability is associated with several pathways such as cell cycle arrest, apoptosis and DNA repair. Low levels of DNA damage appear to enhance p53-dependent DNA repair while high levels induce apoptosis [30]. We envisage that NNK treatments plus radiation at the highest dose introduce genotoxic damage to the cells, the levels of which are enough to trigger the apoptosis. Zhou et al. [31] examined the combined effects of NNK and α-particle irradiation with human–hamster hybrid cultured cells and concluded that the induction of chromosome deletions were additive when the NNK dose was low but a suppressive effect was observed at a higher NNK concentration. In vivo studies also suggest that exposure to high levels of cigarette smoke decrease the risk of lung cancer induced by radon in dogs [32]. However, a multiplicative effect of smoking and radon is observed in rats [33]. In humans, the definitive interaction models have not been established between smoking and radiation exposure [24,25]. Thus, further work is needed to clearly establish the interactive genotoxic mechanisms between radiation and cigarette smoking in vivo.

NNK, a tobacco-specific nitrosamine, is metabolically activated by α-hydroxylation of the methyl and methylene groups [34]. Methylene hydroxylation leads to DNA methylation while methyl hydroxylation leads to pyridyloxobutylated DNA [35]. DNA methylation occurs at N7 and O^6 of guanine and O^4 and O^2 of thymine. It is suggested that O^6-methylguanine (O^6-mG) and pyridyloxobutylated DNA are responsible for G:C to A:T and G:C to T:A mutations, respectively, which activate Ki-*ras* oncogene in the mouse lung tumors induced by NNK [6]. In the present study, G:C to A:T and G:C to T:A mutations were induced by NNK treatments significantly (Table 1). Tiano et al. [36] examined the genotoxicity of NNK in AS52 hamster cells expressing human CYP2A6 and analyzed the induced mutations with the *gpt* gene as a reporter gene for mutations. Because of the lack of O^6-mG methyltransferase in the cell line, about 80% of mutations were G:C to A:T transitions. Interestingly, most of the G:C to A:T transition hotspots occur at the second G of the GGT sequence motif, which is the motif of codon 12 in the Ki-*ras* oncogene [37]. When we define the hotspot as the site where more than four G:C to A:T mutations were identified, we identified 18 hotspots in the *gpt* gene among 155 G:C to A:T mutants recovered from NNK-treated mice. They are nucleotide 27, 64, 86, 87, 92, 107, 110, 113, 115, 116, 128, 274, 281, 287, 402, 409, 417 and 418 when A of ATG of the start codon of the *gpt* gene is set as nucleotide 1. Tiano et al. [36] identified four hotspots of the second G of GGT in nucleotide 23, 116, 128 and 281 in the *gpt* gene, three of which are included in the hotspots identified by us. However, we identified other hotspots such as the second G of GGA at nucleotide 87, 274, 402 and 418, the second G of GGG at nucleotide 27, 64, 92 and 417 and the second G of GGC at nucleotide 113. Thus, we conclude that NNK preferentially induces G:C to A:T mutations at the second G of GGX where X represents any of A, T, G and C. In addition to G:C to A:T and G:C to T:A mutations, we observed an increase in the MFs of A:T to T:A and A:T to C:G in the NNK treated mice (Table 1). Substantial increases in the MFs of A:T to T:A and A:T to C:G are also reported by Hashimoto et al. [38], who examined the genotoxicity of NNK with *lacZ* transgenic mice (Muta^{TM} Mouse). Since reporter genes for mutations, such as *gpt*, *cII* or *lacZ*, are not expressed in vivo and are not imposed by any selection bias, they can reflect any genotoxic events occurring in the genomic DNA. In contrast, oncogenes such as the *ras* gene can only detect mutations that can activate the oncogenic activity of the gene products. Thus, we assume that NNK induces modifications in DNA such as O^4-methyl or O^2-methyl thymine in the lung, which may account for the induction of A:T to C:G and A:T to T:A mutations, respectively [8]. Although the toxicological significance of these mutations is currently unknown, these mutations may contribute to the carcinogenicity of cigarette smoke as well.

γ-Irradiation at dose rate of 1.0 and 1.5 mGy/h clearly enhanced the MFs of large deletions when no NNK treatments were combined (Fig. 3A). The total estimated doses were 0.68 and 1.02 Gy, which may be the lowest radiation doses that gave positive results in transgenic mice mutation assays [16]. In contrast, we could detect no significant increase in the MF of large deletions induced by NNK treatments (Table 2 and Fig. 3A and B). Thus, we suggest that NNK induces mostly base substitutions but not deletions in vivo. Interestingly, NNK treatments induce deletions in cultured mammalian cells. Tiano et al. [36] report that about 20% of mutations induced by NNK treatments are deletions in AS52 hamster cells expressing human CYP2A6. Zhou et al. [31] report that about 80% of NNK-induced mutations are large deletions in the human–hamster hybrid (A_L) cell assay. We speculate that NNK may have a potential to induce both base substitutions and large deletions in vitro but the latter can be eliminated in vivo by the p53-dependent mechanism. Chinese hamster cell lines such as CHO and V79 harbor missense mutation in the *p53*

gene [39,40]. Large deletions might have been detected in the cultured cells because of inefficient p53 functions.

In summary, we have examined the combined genotoxicity of γ-irradiation and NNK treatments in the lung of *gpt* delta mice. Although radiation did not modulate the NNK-induced base substitutions, NNK treatments suppressed the induction of large deletions in size more than 1 kb induced by the irradiation. NNK treatments might induce an adaptive response, which eliminates the cells bearing radiation-induced DSBs in DNA. This finding may be helpful in understanding the molecular mechanisms of genotoxicity as a result of interactions of more than one genotoxic agents in vivo.

Acknowledgements

Part of this study was financially supported by the Budget for Nuclear Research of the Ministry of Education, Culture, Sports, Science and Technology, based on the screening and counseling by the Atomic Energy Commission, and the Tutikawa Memorial Fund for Study in Mammalian Mutagenicity.

References

[1] R. Doll, R. Peto, The causes of cancer: quantitative estimates of avoidable risks of cancer in the United States today, J. Natl. Cancer Inst. 66 (1981) 1191–1308.

[2] Tobacco smoke and involuntary smoking, IARC Monogr Eval. Carcinog. Risk Chem. Hum., vol. 83, International Agency for Research on Cancer, Lyon, France, 2002.

[3] S.S. Hecht, Biochemistry, biology, and carcinogenicity of tobacco-specific *N*-nitrosamines, Chem. Res. Toxicol. 11 (1998) 559–603.

[4] S.S. Hecht, Tobacco carcinogens, their biomarkers and tobacco-induced cancer, Nat. Rev. Cancer 3 (2003) 733–744.

[5] International Agency for Research on Cancer Press Release, vol. 154, International Agency for Research on Cancer, Lyon, France, 2004.

[6] Z.A. Ronai, S. Gradia, L.A. Peterson, S.S. Hecht, G to A transitions and G toT transversions in codon 12 of the Ki-*ras* oncogene isolated from mouse lung tumors induced by 4-(methylnitrosamino)-1-(3-pyridyl)-1-butanone (NNK) and related DNA methylating and pyridyloxobutylating agents, Carcinogenesis 14 (1993) 2419–2422.

[7] R. Guza, M. Rajesh, Q. Fang, A.E. Pegg, N. Tretyakova, Kinetics of O^6-methyl-2′-deoxyguanosine repair by O^6-alkylguanine DNA alkyltransferase within *K-ras* gene-derived DNA sequences, Chem. Res. Toxicol. 19 (2006) 531–538.

[8] E.C. Friedberg, G.C. Walker, W. Siede, R.D. Wood, R.A. Schultz, T. Ellenberger, DNA Repair and Mutagenesis, 2nd ed., ASM Press, Washington, DC, 2006, pp. 1–1118.

[9] United Nations Scientific Committee on the Effects of Atomic Radiation, Sources, Effects and Risks of Ionising Radiation, 1988 Report to the General Assembly with Annexes, United Nations Press, New York, 1989.

[10] J.H. Lubin, K. Steindorf, Cigarette use and the estimation of lung cancer attributable to radon in the United States, Radiat. Res. 141 (1995) 79–85.

[11] H.P. Leenhouts, M.J. Brugmans, Calculation of the 1995 lung cancer incidence in The Netherlands and Sweden caused by smoking and radon: risk implications for radon, Radiat. Environ. Biophys. 40 (2001) 11–21.

[12] United Nations Scientific Committee on the Effects of Atomic Radiation, Combined Effects of Radiation and Other Agents, Report to the General Assembly, United Nations Press, New York, 1998.

[13] M.S. Sasaki, Y. Ejima, A. Tachibana, T. Yamada, K. Ishizaki, T. Shimizu, T. Nomura, DNA damage response pathway in radioadaptive response, Mutat. Res. 504 (2002) 101–118.

[14] T. Lindahl, B. Sedgwick, M. Sekiguchi, Y. Nakabeppu, Regulation and expression of the adaptive response to alkylating agents, Annu. Rev. Biochem. 57 (1988) 133–157.

[15] N.G. Oliveira, M. Neves, A.S. Rodrigues, G.O. Monteiro, T. Chaveca, J. Rueff, Assessment of the adaptive response induced by quercetin using the MNCB peripheral blood human lymphocytes assay, Mutagenesis 15 (2000) 77–83.

[16] T. Nohmi, K.I. Masumura, *gpt* Delta transgenic mouse: a novel approach for molecular dissection of deletion mutations in vivo, Adv. Biophys. 38 (2004) 97–121.

[17] T. Nohmi, T. Suzuki, K. Masumura, Recent advances in the protocols of transgenic mouse mutation assays, Mutat. Res. 455 (2000) 191–215.

[18] M. Miyazaki, H. Yamazaki, H. Takeuchi, K. Saoo, M. Yokohira, K. Masumura, T. Nohmi, Y. Funae, K. Imaida, T. Kamataki, Mechanisms of chemopreventive effects of 8-methoxypsoralen against 4-(methylnitrosamino)-1-(3-pyridyl)-1-butanone-induced mouse lung adenomas, Carcinogenesis 26 (2005) 1947–1955.

[19] T. Nohmi, M. Suzuki, K. Masumura, M. Yamada, K. Matsui, O. Ueda, H. Suzuki, M. Katoh, H. Ikeda, T. Sofuni, Spi$^-$ selection: an efficient method to detect gamma-ray-induced deletions in transgenic mice, Environ. Mol. Mutagen. 34 (1999) 9–15.

[20] K. Masumura, K. Kuniya, T. Kurobe, M. Fukuoka, F. Yatagai, T. Nohmi, Heavy-ion-induced mutations in the *gpt* delta transgenic mouse: comparison of mutation spectra induced by heavy-ion, X-ray, and gamma-ray radiation, Environ. Mol. Mutagen. 40 (2002) 207–215.

[21] T. Nohmi, K. Masumura, Molecular nature of intrachromosomal deletions and base substitutions induced by environmental mutagens, Environ. Mol. Mutagen. 45 (2005) 150–161.

[22] M. Horiguchi, K.I. Masumura, H. Ikehata, T. Ono, Y. Kanke, T. Nohmi, Molecular nature of ultraviolet B light-induced deletions in the murine epidermis, Cancer Res. 61 (2001) 3913–3918.

[23] W. Zhang, C. Wang, D. Chen, M. Minamihisamatsu, H. Morishima, Y. Yuan, L. Wei, T. Sugahara, I. Hayata, Effect of smoking on chromosomes compared with that of radiation in the residents of a high-background radiation area in China, J. Radiat. Res. (Tokyo) 45 (2004) 441–446.

[24] Z.B. Tokarskaya, B.R. Scott, G.V. Zhuntova, N.D. Okladnikova, Z.D. Belyaeva, V.F. Khokhryakov, H. Schollnberger, E.K. Vasilenko, Interaction of radiation and smoking in lung cancer induction among workers at the Mayak nuclear enterprise, Health Phys. 83 (2002) 833–846.

[25] V.E. Archer, Enhancement of lung cancer by cigarette smoking in uranium and other miners, Carcinog. Compr. Surv. 8 (1985) 23–37.

[26] K. Sakai, Y. Hoshi, T. Nomura, T. Oda, T. Iwasaki, K. Fujita, T. Yamada, H. Tanooka, Suppression of carcinogenic processes in mice by chronic low dose rate gamma-irradiation, Int. J. Low Radiat. 1 (2003) 142–146.
[27] S. Wolff, Failla memorial lecture. Is radiation all bad? The search for adaptation, Radiat. Res. 131 (1992) 117–123.
[28] J.D. Tucker, K.J. Sorensen, C.S. Chu, D.O. Nelson, M.J. Ramsey, C. Urlando, J.A. Heddle, The accumulation of chromosome aberrations and *Dlb-1* mutations in mice with highly fractionated exposure to gamma radiation, Mutat. Res. 400 (1998) 321–335.
[29] C.E. Canman, M.B. Kastan, Role of p53 in apoptosis, Adv. Pharm. 41 (1997) 429–460.
[30] H. Offer, N. Erez, I. Zurer, X. Tang, M. Milyavsky, N. Goldfinger, V. Rotter, The onset of p53-dependent DNA repair or apoptosis is determined by the level of accumulated damaged DNA, Carcinogenesis 23 (2002) 1025–1032.
[31] H. Zhou, L.X. Zhu, K. Li, T.K. Hei, Radon, tobacco-specific nitrosamine and mutagenesis in mammalian cells, Mutat. Res. 430 (1999) 145–153.
[32] F.T. Cross, R.F. Palmer, R.E. Filipy, G.E. Dagle, B.O. Stuart, Carcinogenic effects of radon daughters, uranium ore dust and cigarette smoke in beagle dogs, Health Phys. 42 (1982) 33–52.
[33] F.T. Cross, Radioactivity in cigarette smoke issue, Health Phys. 46 (1984) 205–208.
[34] S.S. Hecht, D. Hoffmann, Tobacco-specific nitrosamines, an important group of carcinogens in tobacco and tobacco smoke, Carcinogenesis 9 (1988) 875–884.
[35] Y. Lao, P.W. Villalta, S.J. Sturla, M. Wang, S.S. Hecht, Quantitation of pyridyloxobutyl DNA adducts of tobacco-specific nitrosamines in rat tissue DNA by high-performance liquid chromatography-electrospray ionization-tandem mass spectrometry, Chem. Res. Toxicol. 19 (2006) 674–682.
[36] H.F. Tiano, R.L. Wang, M. Hosokawa, C. Crespi, K.R. Tindall, R. Langenbach, Human CYP2A6 activation of 4-(methylnitrosamino)-1-(3-pyridyl)-1-butanone (NNK): mutational specificity in the *gpt* gene of AS52 cells, Carcinogenesis 15 (1994) 2859–2866.
[37] L.A. Peterson, S.S. Hecht, O^6-Methylguanine is a critical determinant of 4-(methylnitrosamino)-1-(3-pyridyl)-1-butanone tumorigenesis in A/J mouse lung, Cancer Res. 51 (1991) 5557–5564.
[38] K. Hashimoto, K. Ohsawa, M. Kimura, Mutations induced by 4-(methylnitrosamino)-1-(3-pyridyl)-1-butanone (NNK) in the *lacZ* and *cII* genes of Muta Mouse, Mutat. Res. 560 (2004) 119–131.
[39] H. Lee, J.M. Larner, J.L. Hamlin, Cloning and characterization of Chinese hamster p53 cDNA, Gene 184 (1997) 177–183.
[40] W. Chaung, L.J. Mi, R.J. Boorstein, The p53 status of Chinese hamster V79 cells frequently used for studies on DNA damage and DNA repair, Nucl. Acids Res. 25 (1997) 992–994.

Available online at www.sciencedirect.com
ScienceDirect
Mutation Research 627 (2007) 78–91
Genetic Toxicology and Environmental Mutagenesis
www.elsevier.com/locate/gentox
Community address: www.elsevier.com/locate/mutres

Report of the IWGT working group on strategies and interpretation of regulatory *in vivo* tests I. Increases in micronucleated bone marrow cells in rodents that do not indicate genotoxic hazards

D.J. Tweats [a,*], D. Blakey [b], R.H. Heflich [c], A. Jacobs [d], S.D. Jacobsen [e], T. Morita [f], T. Nohmi [g], M.R. O'Donovan [h], Y.F. Sasaki [i], T. Sofuni [j], R. Tice [k]

[a] *Centre for Molecular Genetics and Toxicology, University of Wales, Swansea, UK*
[b] *Safe Environments Programme, Health Canada, Ottawa, Canada*
[c] *National Center for Toxicological Research, US FDA, HFT-120, Jefferson, AR 72079, USA*
[d] *Office of New Drugs, Center for Drug Evaluation and Research, U.S. FDA, HFD024, Rockville, MD 20852, USA*
[e] *Novo Nordisk A/S, Novo Nordisk Park, Måløv, Denmark*
[f] *Division of Safety Information on Drug, Food and Chemicals, National Institute of Health Sciences, Tokyo, Japan*
[g] *Division of Genetics and Mutagenesis, National Institute of Health Sciences, Setagaya-ku, Tokyo, Japan*
[h] *Safety Assessment UK, AstraZeneca R&D Alderley Park, Mereside, Macclesfield, Cheshire, UK*
[i] *Hachinohe National College of Technology, Hachinohe, Aomori, Japan*
[j] *Division of Genetics and Mutagenesis, National Institute of Health Sciences, Setagaya-ku, Tokyo, Japan*
[k] *National Institute of Environmental Health Sciences, EC-17, Research Triangle Park, NC 27709, USA*

Received 28 February 2006; received in revised form 31 July 2006; accepted 14 August 2006
Available online 20 November 2006

Abstract

In vivo genotoxicity tests play a pivotal role in genotoxicity testing batteries. They are used both to determine if potential genotoxicity observed *in vitro* is realised *in vivo* and to detect any genotoxic carcinogens that are poorly detected *in vitro*. It is recognised that individual *in vivo* genotoxicity tests have limited sensitivity but good specificity. Thus, a positive result from the established *in vivo* assays is taken as strong evidence for genotoxic carcinogenicity of the compound tested. However, there is a growing body of evidence that compound-related disturbances in the physiology of the rodents used in these assays can result in increases in micronucleated cells in the bone marrow that are not related to the intrinsic genotoxicity of the compound under test. For rodent bone marrow or peripheral blood micronucleus tests, these disturbances include changes in core body temperature (hypothermia and hyperthermia) and increases in erythropoiesis following prior toxicity to erythroblasts or by direct stimulation of cell division in these cells. This paper reviews relevant data from the literature and also previously unpublished data obtained from a questionnaire devised by the IWGT working group. Regulatory implications of these findings are discussed and flow diagrams have been provided to aid in interpretation and decision-making when such changes in physiology are suspected.

Keywords: IWGT; Genotoxicity tests; *In vivo*; Rodent bone marrow; Micronucleus; Specificity; False positive; Changes in physiology; Hypothermia; Hyperthermia; Spindle disruption; Erythropoiesis; Bone marrow cell toxicity; Pharmacologically related changes; Regulatory implications

* Corresponding author. Tel.: +44 7742 337093
E-mail address: djtweats@fish.co.uk (D.J. Tweats).

1383-5718/$ – see front matter © 2006 Elsevier B.V. All rights reserved.
doi:10.1016/j.mrgentox.2006.10.005

1. Introduction

Established *in vitro* mammalian cell genotoxicity tests, which are used for regulatory testing, have the benefit of high sensitivity for the detection of genotoxic human carcinogens [1]. They also have the disadvantage of less than optimum specificity in terms of their ability to correctly identify non-genotoxic carcinogens and non-carcinogens as negatives. This has been brought into sharp focus by the recent paper of Kirkland et al. [2]. Thus, established *in vivo* genotoxicity assays, such as the rodent bone marrow micronucleus test, are often used to put positive results from *in vitro* genotoxicity assays into perspective, i.e., to determine if the potential of a test compound to induce genotoxic damage *in vitro* is realised in the whole animal where adsorption, distribution, metabolism and excretion are fully functional. Metabolism, including detoxification, is often a key feature in determining the genotoxicity of test agents and metabolic activation may be different *in vivo* compared to *in vitro*. In some apparently rare circumstances the exogenous metabolism provided by rat liver S9, especially from animals pre-treated by cytochrome P450 inducers may be inadequate or inappropriate, so that inherent genotoxicity may be missed *in vitro* (see accompanying paper).

The *in vivo* micronucleus assay, using either bone marrow or peripheral blood, is the focus of this paper. The assay has proved useful for the detection of agents that induce chromosomal damage as: (i) the endpoint is easy to score, (ii) it provides good statistical power as many cells can be scored for the presence of micronuclei, and (iii) there is evidence that chromosomal breakage always leads to micronucleus formation, thus, if the micronucleus test is negative (and the compound and/or its metabolites can be shown to reach the bone marrow), chromosomal aberrations in this tissue can be ruled out. The converse is not true, thus, if the micronucleus assay is positive, one cannot conclude that the mechanism is due to chromosomal breakage without further experiments as will be shown below.

The rodent bone marrow micronucleus test is perceived as having moderate sensitivity for the detection of carcinogens, in that not all genotoxic agents or genotoxic metabolites necessarily reach the bone marrow in sufficient quantities to produce a detectable genotoxic response; however, specificity is perceived to be relatively high, i.e., false positives are apparently rare. Thus, with the regulatory genotoxicity test batteries currently in use, the results of *in vivo* genotoxicity tests, in particular bone marrow cytogenetic tests, play a vital role in risk and hazard assessments. Increases in micronucleated bone marrow cells are given great regulatory weight indicating that the test compound is likely to be a genotoxic carcinogen. However, there is an increasing body of evidence demonstrating that some disturbances in the physiology of treated animals can give rise to apparent increases in cytogenetic damage in the bone marrow that are not due to compound-induced genotoxic damage *per se*. An IWGT Working Group was formed to assess the existing data from the literature on this subject as well as to evaluate previously unpublished data obtained from a questionnaire sanctioned by the IWGT Steering Committee. The questionnaire (Appendix A) was sent to companies and institutes performing or contracting for genotoxicity studies.

The target cell in the bone marrow micronucleus test is the developing erythroblast. During the formation of enucleated erythrocytes, at the final cell division of the erythroblast, the nuclear contents fragment in a process similar to that in apoptotic cells (karyorrhexis) [3] and these fragments are collectively expelled from the cell envelope, contained in a plasma membrane. This is an efficient process, but occasionally some material is left behind in the immature erythrocyte. In haematology, these fragments are termed Howell-Jolly bodies and constitute at least a part of the spontaneous micronuclei seen in cells from untreated animals. Conditions that can reduce oxygen tension in the blood can stimulate the secretion of additional erythropoietin (EPO), which stimulates an increase in cell division of erythroblasts, and hence, increases the numbers of circulating erythrocytes. This improves the overall oxygen carrying capacity of the blood and restores levels of oxygen tension [4]. The increase in cell division will cause more cells to undergo enucleation and this may result in an increase in micronuclei formed 'spontaneously'.

2. Consequences of significant changes in core body temperature

2.1. Cytogenetic effects of hyperthermia and hypothermia in vitro and in vivo

Non-physiological temperatures have been known for some time to induce cytogenetic damage [5]. Transient hyperthermia (40 °C for 24 h or 42 °C for 6 h) induces chromosomal aberrations and micronuclei in CHL cells *in vitro* [6]. This damage is related to the disruption of the mitotic spindle as treatment of dividing cells at 45.5 °C for 5–15 min results in disassembly of the spindle apparatus and disruption of the contractile ring and midbody–cytoplasmic bridge complex [7]. Mild heat shock causes loss of dynamitin/p50 antibody staining from centrosomes and kinetochores. Hsp70 is rapidly

recruited to centromeres following heat shock as a protective measure [8].

Similar effects of hyperthermia occur *in vivo*. Up to four-fold increases in micronucleated erythrocytes have been reported in the bone marrow of mice subjected to whole body hyperthermia of 35–36 °C for 20–32 h [9,10] or 40 °C for 1–2 h [11]. About 25% of the micronuclei were relatively large suggesting the possible presence of whole chromosomes. Thus, it appears that body temperatures of 39.5 °C or higher for more than 30 min induce micronuclei in bone marrow cells due to disturbance of the mitotic apparatus.

Transient hypothermia also induces micronuclei (but not chromosomal damage) in CHL cells (31 or 33 °C for 24 h) [6]. More support for the ability of hypothermia to induce micronuclei comes from the studies of chemically induced hypothermia that are outlined below.

2.2. *Cytogenetic effects of compound-induced hypothermia in the bone marrow micronucleus test*

2.2.1. *Chlorpromazine*

Hypothermia is a known side effect of the binding of neuroleptic drugs to several classes of pharmologically active sites, including dopamine, serotonin, alpha 2 adrenergic receptor and sigma binding sites [12]. Chlorpromazine is one such drug. This phenothiazine compound is negative in assays for gene mutation in bacteria, for chromosome aberrations in mammalian cells and in Drosophila (SLRLT and SMART assays). Analysis of these results suggests that this compound generally is not considered to be a genotoxic agent [13].

Asanami and co-workers carried out a series of mouse bone marrow micronucleus tests on this drug. Doses of 12.5–100 mg/kg chlorpromazine decrease rectal temperature in mice from 37.7 °C to a mean of about 29 °C at 8–11 h after dosing; with the lower doses, body temperature returns to normal after 24 h [6]. Doses of 25–100 mg/kg chlorpromazine produce a significant increase in micronucleated polychromatic erythrocytes (PCEs) at 48 h after dosing (occasional increases were seen for individual doses at 24–48 h). Typical increases were 2.6 micronucleated PCEs/1000 PCEs, in the 100 mg/kg group, compared to 0.8 micronucleated PCEs/1000 PCEs in the controls.

No increases in micronuclei were seen when mice were given 25, 50 or 100 mg/kg chlorpromazine in an environment where the temperature was maintained at 30 °C for 46 h to help keep body temperature in the normal range. This observation provides evidence that the micronuclei seen in chlorpromazine-treated mice were a result of chlorpromazine-induced hypothermia and were not due to another type of inherent genotoxicity of this compound.

In addition, 53–58% of the micronuclei detected in the chlorpromazine-treated animals were relatively large (diameter equal or greater than 0.25 the diameter of the cytoplasm), providing some evidence that the micronuclei were a result of dysfunction of chromosome linkage to the spindle apparatus. It is also possible that hypothermia reduces the oxygen tension of the blood, inducing a stimulation of erythropoietin release and increased cell division of erythroblasts. This could cause an increase in micronucleus formation due to increased rates of cells undergoing enucleation (see Section 1).

Rats are known to be more refractory to the hypothermic effects of phenothiazine drugs such as chlorpromazine. Male SD rats were dosed i.p. with 31.3–250 mg/kg chlorpromazine. This treatment resulted in a decrease in rectal temperature, but only at 250 mg/kg chlorpromazine did the temperature fall below 33 °C for 20 h. This dose also produced a significant increase in micronucleated PCEs (control 0.55/1000 PCEs, test 1.5/1000 PCEs) [14].

2.2.2. *Reserpine*

Reserpine is another phenothiazine, neuroleptic drug. This compound is negative for chromosome aberration induction *in vitro*. Although reserpine has been reported to transform SHE cells, no cytogenetic abnormalities (or other genotoxic effects) were observed [15].

Mouse bone marrow micronucleus tests were conducted with reserpine doses of 1, 4, 10, 100 and 1000 mg/kg and significant increases in micronucleated PCEs were detected 48, 72 and 96 h after treatment with 100 and 1000 mg/kg (controls, 1.5/1000 PCEs, rising to 12/1000 PCEs in the treated animals). These doses produced a decrease in rectal temperature to below 33 °C for the entire 96 h period after dosing, with comparable suppression at 100 and 1000 mg/kg. Temperature suppression was less at 10 mg/kg.

No increases in micronuclei were seen in a study carried out at doses in the range 50–200 mg/kg where the environmental temperature was maintained at 30 °C for 40 h [6].

In rats, which as mentioned for chlorpromazine are more refractory to phenothiazine induced hypothermia, i.p. doses of 500–2000 mg/kg produced neither significant hypothermia nor increases in micronucleated bone marrow erythrocytes [14].

2.2.3. *E-5824*

E-5824 is a triazole pyridine compound that binds to the sigma-1 receptor [12]. It is an atypical antipsychotic

Table 1
Mouse bone marrow micronucleus test of E5824 with and without heating (48 h data only)[a]

Environmental conditions	Dose E5842 (mg/kg)	PCE/NCE	MNPCEs/ 2000 PCEs
RT	0	0.99	1.7
RT	50	1.08	2.1
RT	100	1.28	1.9
RT	200	1.28	3.4*
Heater[b]	0	1.08	1.8
Heater	50	1.30	1.4
Heater	100	0.98	1.4
Heater	200	1.07	1.1

* Statistically significant at $p < 0.05$; ANOVA, followed by Dunnett's test. Groups of five CD-1 mice were dosed by gavage and the bone marrow sampled at 24 h (data not shown) and 48 h following exposure. RT = room temperature; PCE; polychromatic erythrocyte; NCE = normochromatic erythrocyte; MNPCE = micronucleated PCE.

[a] Data taken from Guzman et al. [12].

[b] Animals were housed in Makrolon cages, internal temperature maintained at 30 °C using a Selecta hot air heater (Model 381).

drug. Ames and mouse lymphoma *tk* tests of E-5824 were negative. An increased incidence of micronucleated PCEs was observed in mouse bone marrow 48 h after exposure to 200 mg/kg E-5824 (but not other doses or sampling times) (Table 1). Rectal temperature measurements showed that the test compound decreased core body temperature by more than 7 °C at 50 mg/kg and by almost 13 °C at 200 mg/kg.

As shown in the table, in the repeat test where the environmental temperature was maintained at 30 °C, the micronucleus response disappeared. Measurements of the size distribution of micronuclei showed that the micronuclei induced at 200 mg/kg were skewed towards larger micronuclei, again suggestive that these represented whole chromosome loss from disruption of chromosomal attachment to the spindle due to hypothermia (and/or due to increased rates of enucleation). There are large numbers of sigma 1 binding sites in the hypothalamus [16], a tissue known to be involved in temperature regulation in mammals.

2.2.4. Phenol

Although phenol has promoter activity in the 2-stage skin carcinogenesis model [17], it is regarded as negative in NTP carcinogenicity studies in rats and mice [18]. A more recent IARC assessment stated that there is inadequate experimental evidence for the carcinogenicity of phenol and as such it is not classifiable [19].

CD mice were given single i.p. doses of phenol up to 500 mg/kg. Lethality was seen above 300 mg/kg. At 300 mg/kg, a significant increase in micronucleated PCEs was observed in both male and female animals at 24 and 48 h after dosing (male data are shown in Table 2). In addition, 300 mg/kg phenol (but not the other doses used) induced a significant and prolonged hypothermia where core body temperature was lowered by 7 °C. The authors surmised this might have been responsible for the increases in micronuclei observed. Comparison of these results for phenol with results evaluated by the Working Group indicates that the response is somewhat higher than with other compounds that induce hypothermia. It would be informative to ascertain if this response can be reversed by maintaining the core body temperature of the treated animals.

2.2.5. Covance compound number 4

Compound number 4 is a CNS drug tested under contract. The genotoxicity data were collected using the questionnaire (see Appendix A). *In vitro* genotoxicity assays of the compound were regarded as negative, although a borderline positive was observed in the Ames test using strain TA100 and the pre-incubation protocol. Uniformly negative results were seen in plate

Table 2
Mouse bone marrow micronucleus test of phenol[a]

Test agent	Dose (mg/kg)	Temperature change[b] (°C)	PCE/NCE at 24 h	MN PCEs/1000 PCEs at 24 h	PCE/NCE at 48 h	MN PCEs/1000 PCEs at 48 h
Vehicle control	0	−1.9	1.8	2.1	1.75	1.4
Phenol	30	−0.1	1.08	4.3	1.93	1.3
Phenol	100	−0.3	1.01	3.1	1.87	1.5
Phenol	200	−7.1	1.01	10.8*	0.61	18.3*
Positive control (cyclophosphamide)	120	−0.3	0.59	79.9*	NT	NT

Data shown is from groups of five male CD1 mice (similar data were obtained from female mice) dosed i.p. and sampled 24 and 48 h after dosing. PCE = polychromatic erythrocyte; NCE = normochromatic erythrocyte; MNPCE = micronucleated PCE.

[a] Data taken from Spencer et al. [20].

[b] Average change over a 48 h observation period, temperature measured by a subcutaneous transponder.

* Significantly different from the negative control by Factorial-Rep ANOVA.